

Structural, magnetic, transport and magnetocaloric properties of metamagnetic DyMn_{0.5}Co_{0.5}O₃

C. Ganeshraj, R. Pradheesh, and P. N. Santhosh

Citation: *J. Appl. Phys.* **111**, 07A914 (2012); doi: 10.1063/1.3672067

View online: <http://dx.doi.org/10.1063/1.3672067>

View Table of Contents: <http://jap.aip.org/resource/1/JAPIAU/v111/i7>

Published by the [American Institute of Physics](#).

Related Articles

Investigation of the hydrogen bonding in ice Ih by first-principles density function methods

J. Chem. Phys. **137**, 044504 (2012)

Effects of Ca-substitution on structural, dielectric, and ferroelectric properties of Ba₅SmTi₃Nb₇O₃₀ tungsten bronze ceramics

Appl. Phys. Lett. **101**, 042906 (2012)

Mg doping in wurtzite ZnO coupled with native point defects: A mechanism for enhanced n-type conductivity and photoluminescence

Appl. Phys. Lett. **101**, 042106 (2012)

Crystal structure, local structure, and defect structure of Pr-doped SrTiO₃

J. Appl. Phys. **112**, 024103 (2012)

First principles investigation of structural, electronic, elastic and thermal properties of rare-earth-doped titanate Ln₂TiO₅

AIP Advances **2**, 032114 (2012)

Additional information on *J. Appl. Phys.*

Journal Homepage: <http://jap.aip.org/>

Journal Information: http://jap.aip.org/about/about_the_journal

Top downloads: http://jap.aip.org/features/most_downloaded

Information for Authors: <http://jap.aip.org/authors>

ADVERTISEMENT



IBD Optical Film Quality at PVD Rates

Advanced Optical Thin Films

Wide Range of Applications

Superior Throughput and Repeatability

SPECTOR-HT ION BEAM DEPOSITION SYSTEMS

Veeco
Innovation. Performance. Brilliant.

www.veeco.com/spectorht

Structural, magnetic, transport and magnetocaloric properties of metamagnetic $\text{DyMn}_{0.5}\text{Co}_{0.5}\text{O}_3$

C. Ganeshraj, R. Pradheesh, P. N. Santhosh^{a)}

Low Temperature Physics Laboratory, Department of Physics, Indian Institute of Technology Madras, Chennai-600 036, Tamilnadu, India

(Presented 2 November 2011; received 22 September 2011; accepted 21 October 2011; published online 22 February 2012)

Rietveld refinement of the powder diffraction data revealed that $\text{DyMn}_{0.5}\text{Co}_{0.5}\text{O}_3$ (DMCO) crystallized in an orthorhombic structure containing distorted Mn/Co– O_6 octahedra (sp.gr = $Pnma$; $a = 5.5922(1)$ Å, $b = 7.4987(1)$ Å, $c = 5.2606(1)$ Å). Below 85 K, the field cooled magnetization data shows a spontaneous magnetic ordering. The metamagnetic behavior of the sample is evident from the nature of variation of magnetization with applied magnetic field. The field dependent magnetization at 5 K, points out the Mn and Co ions are aligned ferromagnetically, whereas Dy and Mn-Co sublattices are coupled antiferromagnetically. The magnitude of isothermal magnetic entropy change, $|\Delta S_{\text{M}}|_{\text{max}}$ is $\sim 9.30 \text{ J kg}^{-1} \text{ K}^{-1}$ in the vicinity of magnetic ordering of Dy^{3+} for the field change of 7 T, is appreciable to consider $\text{DyMn}_{0.5}\text{Co}_{0.5}\text{O}_3$ as a magnetic refrigerant at low temperatures. The temperature variation of electrical resistivity shows the highly insulating nature of the sample. © 2012 American Institute of Physics. [doi:10.1063/1.3672067]

I. INTRODUCTION

Perovskites of the formula $\text{AB}_{1-x}\text{B}'_x\text{O}_3$ ($0 \leq x \leq 1$, where A is rare earth ions and B, B' are transition metal ions) have received great attention because some of them shows colossal magnetoresistance,¹ magnetoelectric,^{2,3} and magnetocaloric effect (MCE).^{4,5} The magnetocaloric effect is intrinsic to all magnetic materials, induced via coupling of the magnetic sublattice with the magnetic field which alters the magnetic part of total entropy due to a corresponding change of the magnetic field.⁶ Magnetic refrigeration, based on MCE, has attracted considerable research interest due to its potential advantage of the higher energy efficiency over the conventional compression refrigeration.⁷ There has been increasing interest in magnetic materials with large magnetocaloric effect over past decade.^{8,9}

The existence of metamagnetic behavior is an uncommon feature in the cobalt manganese compounds. Based on the magnetic measurements, it was reported, $\text{Ln}(\text{Mn}_{1-x}\text{Co}_x)\text{O}_{3+\lambda}$ (Ln = Eu, Nd, Y) series show metamagnetic behavior due to field induced transition from the ferrimagnetic phase, where the magnetic moments of Mn^{4+} and Co^{2+} are antiparallel, to the ferromagnetic phase.¹⁰ In the present work we report the MCE observed in metamagnetic perovskite $\text{DyMn}_{0.5}\text{Co}_{0.5}\text{O}_3$. The compound is found to show insulator behavior and below room temperature the variable range hopping model is found to fit very well.

II. EXPERIMENTAL DETAILS

Polycrystalline sample of $\text{DyMn}_{0.5}\text{Co}_{0.5}\text{O}_3$ was synthesized using a conventional solid state synthesis route. The solid solution was prepared by mixing the stoichiometric mixtures of Dy_2O_3 , MnO_2 , and Co_3O_4 precursors and was homogenized in an agate mortar before it is reacted at 1100 °C. Final sintering was done at 1100 °C. The sample was characterized

by powder X-ray diffraction (XRD) experiments using (PANalytical X'Pert Pro) X-ray diffractometer with Cu K_α radiation. Rietveld refinement for the XRD pattern of $\text{DyMn}_{0.5}\text{Co}_{0.5}\text{O}_3$ was carried out by means of the general structure analysis system (GSAS) package.¹¹ Magnetic measurements were made using a superconducting quantum interference device susceptometer (MPMS, Quantum Design) in fields up to 7 T, in the temperature range 2–300 K. The temperature variation of electrical resistivity was done by two probe method in the temperature range of 80–300 K.

III. RESULTS AND DISCUSSION

A. Crystal structure

The Rietveld analysis of the room temperature XRD data of $\text{DyMn}_{0.5}\text{Co}_{0.5}\text{O}_3$ shows that the sample crystallizes in the orthorhombic structure with space group $Pnma$ in

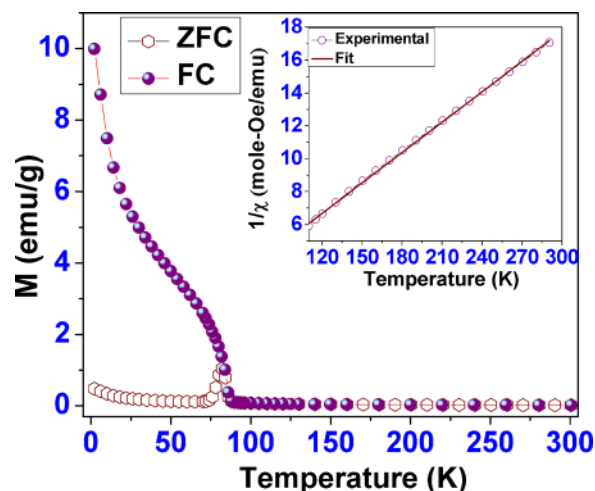


FIG. 1. (Color online) FC and ZFC magnetization vs temperature in an applied field 100 Oe. The inset shows the Curie-Weiss fit.

^{a)}Electronic mail: santhosh@physics.iitm.ac.in. Fax: +91 44 2257 4852.

TABLE I. Lattice parameters, goodness of fit, selected bond lengths, and selected bond angles of $\text{DyMn}_{0.5}\text{Co}_{0.5}\text{O}_3$. Figures in the parentheses are estimated standard deviations referred to the last significant digit.

a (Å)	5.5922(1)
b (Å)	7.4987(1)
c (Å)	5.2606(1)
$\alpha = \beta = \gamma$ (°)	90
χ^2	1.524
W_{RP}	4.01%
Mn/Co-O _a (Å)	1.9571(3) × 2
Mn/Co-O _c (Å)	1.9890(3) × 2
Mn/Co-O _e (Å)	2.0150(3) × 2
Mn/Co-O _e -Mn/Co (°)	146.9(0)
Mn/Co-O _a -Co/Mn (°)	146.6(1)

which the octahedral B cations are disordered. The goodness of fit, refined lattice parameters, bond lengths, and bond angles are given in Table I and the refined structural parameters are given in Table II. The single phase nature of the compound was confirmed by Rietveld analysis.

B. Magnetic properties of $\text{DyMn}_{0.5}\text{Co}_{0.5}\text{O}_3$

The temperature dependence of magnetization of $\text{DyMn}_{0.5}\text{Co}_{0.5}\text{O}_3$, measured at 100 Oe, is shown in Fig. 1. One can observe that spontaneous magnetization begins to develop at $T_C = 85$ K. The zero field cooled (ZFC) curve passes through a maximum slightly below the Curie point and sharply deviates from field cooled (FC) magnetization with decreasing temperature. This kind of behavior of ZFC dependence is characteristic of the cobaltites and is attributed to the large magnetic anisotropy in these compounds.¹² The inverse susceptibility versus temperature follows Curie-Weiss behavior above 120 K as shown in the inset of Fig. 1. The Curie constant C obtained from Curie-Weiss fit suggests that the spin of Dy^{3+} , Co^{2+} , and Mn^{4+} ions give rise to the magnetism in $\text{DyMn}_{0.5}\text{Co}_{0.5}\text{O}_3$.¹³ The paramagnetic Curie temperature $\theta_p \sim 11.50$ K indicative of the presence of ferromagnetic interactions, arises from $\text{Mn}^{4+} - \text{O} - \text{Co}^{2+}$ whereas $\text{Mn}^{4+} - \text{O} - \text{Mn}^{4+}$ and $\text{Co}^{2+} - \text{O} - \text{Co}^{2+}$ interactions are antiferromagnetic in nature.¹⁴ The magnetization versus field dependence for $\text{DyMn}_{0.5}\text{Co}_{0.5}\text{O}_3$ at 5 K, 50 K, and 300 K is presented in Fig. 2. The magnetic moment at 5 K for an applied field of 7 T is $5.61 \mu_B/\text{F.U.}$, indicates that Mn and Co ions are aligned ferromagnetically, whereas Dy and Mn - Co sublattices prefer to align antiferromagnetically.^{13,15} The temperature variation of the real part of ac susceptibility measured at different frequency and dc magnetic fields do not show any shift in ac susceptibility peak position with temperature, ruling out the possible spin glass nature in the system (figure not shown).

TABLE II. Crystal structure parameters of $\text{DyMn}_{0.5}\text{Co}_{0.5}\text{O}_3$.

	x	y	Z	Occupancy
Dy	0.0703	0.2500	0.9852	1
Mn/Co	0	0	0.5	0.5/0.5
O1	0.4662	0.2500	0.1006	1
O2	0.2982	0.0529	0.6917	1

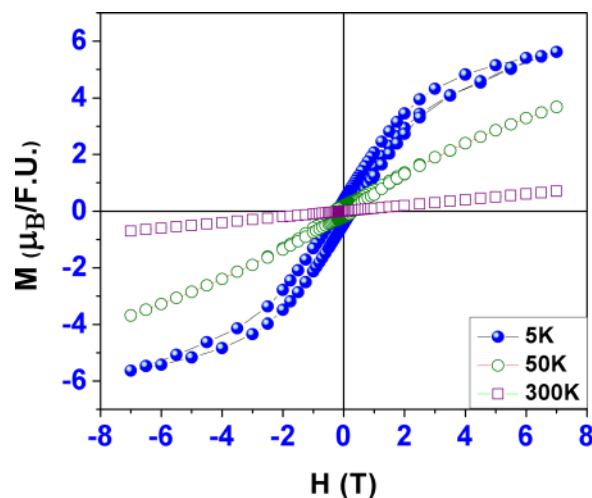


FIG. 2. (Color online) Curves of M vs H at 5 K, 50 K, and 300 K.

C. Metamagnetic behavior of $\text{DyMn}_{0.5}\text{Co}_{0.5}\text{O}_3$

Figure 3 depicts the field dependent magnetization curves measured at 20 K, 40 K, and 60 K. They clearly show an applied field induced metamagnetic transition from the ferrimagnetic state, where Mn^{4+} and Co^{2+} magnetic moments are antiparallel, to the ferromagnetic state where they are parallel.¹⁰ Similar kinds of features have been observed in $\text{TbCo}_{0.5}\text{Mn}_{0.5}\text{O}_{3.06}$ and similar magnetic coupling is evident in neutron diffraction data.¹³

D. Magnetocaloric effect of $\text{DyMn}_{0.5}\text{Co}_{0.5}\text{O}_3$

In order to calculate the magnetic entropy change (ΔS_M), which results from magnetic ordering, we have measured various M - H isotherms from 5 K to 40 K and 60 K to 140 K. According to Maxwell's thermodynamic relation, $(\partial S/\partial H)_T = (\partial M/\partial T)_H$, the change in magnetic entropy ΔS_M is given by $\Delta S_M(T, M) = S_M(T, M) - S_M(T, 0) = \int_0^H (\partial M/\partial T)_H dH$ and is calculated by the variation of a magnetic field from 0 to H .¹⁶ Figure 4 shows the magnetic entropy change as a function of

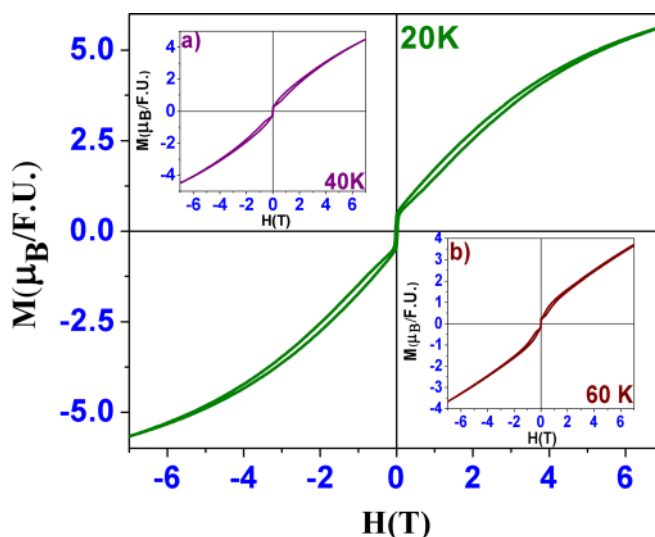


FIG. 3. (Color online) Field dependent magnetization at 20 K. Inset shows field dependent magnetization at (a) 40 K and (b) 60 K.

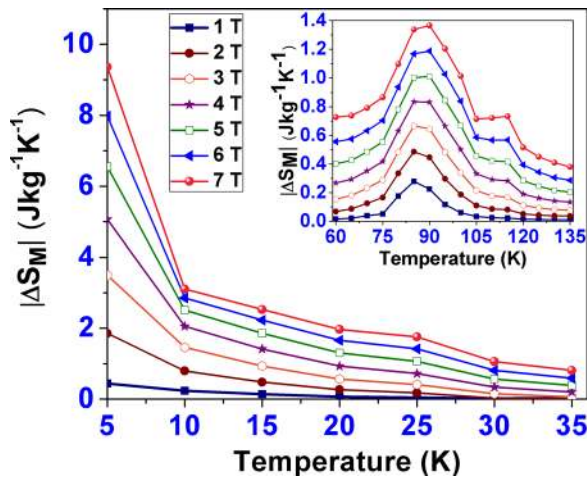


FIG. 4. (Color online) Magnetic entropy change of $\text{DyMn}_{0.5}\text{Co}_{0.5}\text{O}_3$ from 5 K to 40 K at various magnetic fields. The inset shows magnetic entropy change of $\text{DyMn}_{0.5}\text{Co}_{0.5}\text{O}_3$ from 60 K to 140 K at various magnetic fields.

temperature from 5 K to 40 K. The maximum $|\Delta S_M|$ value is $\sim 9.30 \text{ J kg}^{-1} \text{ K}^{-1}$ for a field change of 7 T, around 5 K. This is close to the magnetic ordering temperature of Dy^{3+} ions.¹⁷ A small peak around 25 K indicates the Mn/Co spin reorientation. The inset of Fig. 4 displays the obtained $|\Delta S_M|$ as a function of temperature from 60 K to 140 K under applied fields. A peak around 85 K shows the magnetic ordering of Mn/Co ions. One can note that a $|\Delta S_M|$ peak, around 85 K, gradually broadens to the higher temperature while increasing field, is due to the field-induced metamagnetic transition.¹⁸

E. Transport properties of $\text{DyMn}_{0.5}\text{Co}_{0.5}\text{O}_3$

The temperature dependence of electrical resistivity (ρ) of $\text{DyMn}_{0.5}\text{Co}_{0.5}\text{O}_3$ measured from 80 K to 300 K is shown in Fig. 5. With decreasing temperature the resistivity increases and the value is very high at low temperature, shows the insulating behavior of $\text{DyMn}_{0.5}\text{Co}_{0.5}\text{O}_3$. Around 100 K the resistivity value starts increasing rapidly, due to spontaneous ordering of Mn/Co ions. The temperature dependence of resistivity of the compound could best fit to Mott variable-range hopping

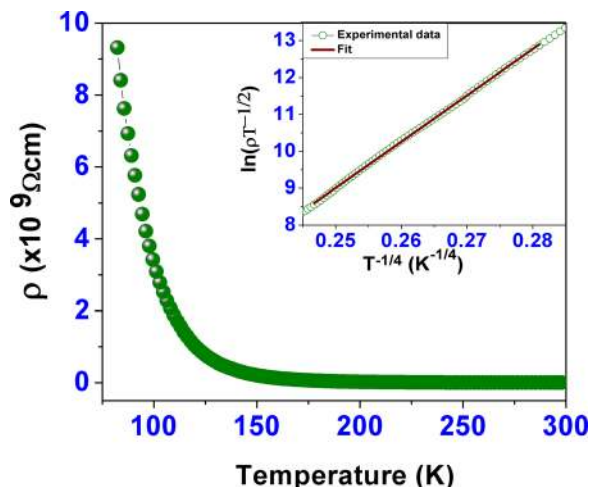


FIG. 5. (Color online) Electrical resistivity vs temperature of $\text{DyMn}_{0.5}\text{Co}_{0.5}\text{O}_3$. Inset: VRH model fit.

(VRH) behavior¹⁹ of the form $\rho = \rho_0 (T/T_0)^{1/2} \exp (T_0/T)^{1/4}$, where $k_B T_0$ is mean energy difference between the localized states which is spatially separated by one localization length that is $k_B T_0 = 4\nu_c [g(\epsilon_F) \xi^3]^{-1}$, where $g(\epsilon_F)$ is the density of the states at the Fermi energy, ξ ($\sim 10 \text{ \AA}$) is the localization length, and ν_c is the dimensionless constant. The linear fit for $\ln(\rho T^{-1/2})$ versus $T^{-1/4}$ (3 D hopping) is plotted in the inset of Fig. 5. The value of $g(\epsilon_F)$ obtained from the fit is $7.472 \times 10^{18} \text{ eV}^{-1} \text{ cm}^{-3}$. The value of $g(\epsilon_F)$ matches with the usual oxide semiconductor [$g(\epsilon_F) \sim 10^{17} - 10^{19} \text{ eV}^{-1} \text{ cm}^{-3}$].¹⁹

IV. CONCLUSION

The polycrystalline $\text{DyMn}_{0.5}\text{Co}_{0.5}\text{O}_3$ prepared by the solid state reaction method is found to be formed in orthorhombic structure. The sample undergoes a magnetic transition around 85 K and also shows a metamagnetic behavior. MCE is calculated from magnetization data and maximum isothermal magnetic entropy change of $\sim 9.30 \text{ J kg}^{-1} \text{ K}^{-1}$ is observed around 5 K for a field change of 7 T and the compound may be considered as a magnetic refrigerant at low temperatures. The resistivity data shows the insulating nature of the compound and the variable range hopping model is found to be valid below room temperature.

ACKNOWLEDGMENTS

It is a pleasure to acknowledge Dr. R. Nirmala for helpful discussions on the magnetocaloric effect. This work was supported by Department of Science and Technology, India for financial assistance [Multiferroics project (SR/S2/CMP-25/2005)].

¹K. L. Kobayashi, T. Kimura, H. Sawada, K. Terakura, and Y. Tokura, *Nature* **395**, 677 (1998).

²D. I. Khomskii, *J. Magn. Magn. Mater.* **306**, 1 (2006).

³Z.G. Ye and Schmid, *Ferroelectrics* **162**, 119 (1994).

⁴Jinhua Mao, Yu Sui, Xingquan Zhang, Yantao Su, Xianjie Wang, Zhiguo Liu, Yi Wang, Ruibin Zhu, Yang Wang, Wanfa Liu, and Jinke Tang, *Appl. Phys. Lett.* **98**, 192510 (2011).

⁵M. El-Hagary, *J. Alloys Compd.* **502**, 376 (2010).

⁶A. M. Tishin and Y. L. Spichikn, *The Magnetocaloric Effect and Its Applications*. (Institute of Physics, Cornwall, 2003).

⁷F.O. Tegus, E. Beruk, K. H. Bushow, and F. R. de Boer, *Nature (London)* **415**, 150 (2002).

⁸V. K. Perchasky and Gschneidner, *Phys. Rev. Lett.* **78**, 4494 (1997).

⁹Y. Sun, X. Xu, and Y. Zhang, *J. Magn. Magn. Mater.* **219**, 183 (2000).

¹⁰I. O. Troyanchuk, D. D. Khalyavin, J. W. Lunn, R. W. Erwin, Q. Huang, H. Szymczak, R. Szymczak, and M. Baran, *J. Appl. Phys.* **88**, 360 (2000).

¹¹A. C. Larson and R. B. Von Dreele, "General Structure Analysis System (GSAS)," Los Alamos National Laboratory Report No. LAUR 86-748 (1994).

¹²R. Ganguly, A. Maignan, C. Martin, M. Hervieu, and B. Raveau, *J. Phys.: Condens. Matter*, **14**, 8595 (2002).

¹³V. A. Khomchenko, I. O. Troyanchuk, A. P. Sazonov, V. V. Sikolenko, H. Szymczak, and R. Szymczak, *J. Phys.: Condens. Matter* **18**, 9541 (2006).

¹⁴I. O. Troyanchuk, N. V. Samsonenko, A. Nabiaiek, and H. Szymczak, *J. Magn. Magn. Mater.* **168**, 309 (1997).

¹⁵P. Aleshkevych, M. Baran, S. N. Barilo, V. I. Gatal'skaya, S. V. Shiryayev, R. Szymczak, and H. Szymczak, *Phys. Status Solidi B* **243**, 263 (2006).

¹⁶M. Foldeaki, R. Chahine, and T. K. Bose, *J. Appl. Phys.* **77**, 3528 (1995).

¹⁷S. Harikrishnan, S. Rößler, C. M. Naveen Kumar, H. L. Bhat, U. K. Rößler, S. Wirth, F. Steglich, and Suja Elizabeth, *J. Phys.: Condens. Matter* **21**, 096002 (2009).

¹⁸V. Suresh Kumar and R. Mahendiran, *Solid State Commun.* **150**, 1445 (2010).

¹⁹N. F. Mott, *J. Non-Cryst. Solids* **1**, 1 (1968).